



저작자표시-비영리-변경금지 2.0 대한민국

이용자는 아래의 조건을 따르는 경우에 한하여 자유롭게

- 이 저작물을 복제, 배포, 전송, 전시, 공연 및 방송할 수 있습니다.

다음과 같은 조건을 따라야 합니다:



저작자표시. 귀하는 원저작자를 표시하여야 합니다.



비영리. 귀하는 이 저작물을 영리 목적으로 이용할 수 없습니다.



변경금지. 귀하는 이 저작물을 개작, 변형 또는 가공할 수 없습니다.

- 귀하는, 이 저작물의 재이용이나 배포의 경우, 이 저작물에 적용된 이용허락조건을 명확하게 나타내어야 합니다.
- 저작권자로부터 별도의 허가를 받으면 이러한 조건들은 적용되지 않습니다.

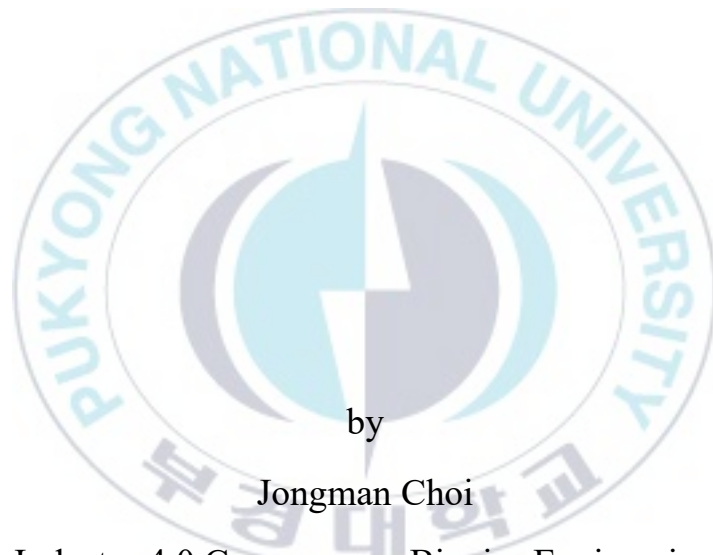
저작권법에 따른 이용자의 권리는 위의 내용에 의하여 영향을 받지 않습니다.

이것은 [이용허락규약\(Legal Code\)](#)을 이해하기 쉽게 요약한 것입니다.

[Disclaimer](#)

Thesis for the Degree of Master of Engineering

**Development of Diffractive Micro-Lens Array
(DLA) based on picosecond Nd:YAG laser for
skin treatment**



by

Jongman Choi

Industry 4.0 Convergence Bionics Engineering

The Graduate School

Pukyong National University

February 2023

Development of Diffractive Micro-Lens Array (DLA) based on picosecond Nd:YAG laser for skin treatment

(색소 병변 치료 및 피부 재생을 위한
피코초 엔디야그레이저 기반 회절 마이크로
렌즈 어레이(DLA) 개발 연구)

Advisor: Prof. Hyun Wook Kang

by

Jongman Choi

A thesis submitted in partial fulfillment of the requirements
for the degree of
Master of Engineering

Industry 4.0 Convergence Bionics Engineering,
The Graduate School,
Pukyong National University

February 2023

Development of Diffractive Micro-Lens Array (DLA) based on picosecond
Nd:YAG laser for skin treatment

A dissertation

by

Jongman Choi

Approved by:



(Chairman) Yi Myunggi Ph. D



(Member) Junghwan Oh Ph. D



(Member) Hyun Wook Kang Ph. D

February 17, 2023

**Development of Diffractive Micro-Lens Array (DLA) based on picosecond Nd:YAG
laser for skin treatment**

Jongman Choi

Industry 4.0 Convergence Bionics Engineering

The Graduate School

Pukyong National University

Abstract

현대사회에 들어 인류 삶의 질 향상과 함께 심미적 가치 증가함에 따라 피부 관련 색소 치료와 재생 분야의 수요가 증가하고 있다. 피코초 엔디야그 레이저(Picosecond Nd:YAG Laser)는 대표적인 피부 치료용 레이저 중 하나로, 피부 색소 치료와 피부 재생 분야에 널리 사용되고 있다. 특히 피코초 엔디야그 레이저는 수백 피코초 단위의 짧은 펄스폭을 특징으로 회절 광학 소자(Diffractive optical element, DOE) 및 마이크로 렌즈 어레이(Micro lens array, MLA)와 함께 쓰여, 피하에 다중 미세 레이저 빔을 형성함과 동시에 레이저 유도 광학적 파괴(Laser induced optical breakdown, LIOB)를 일으킬 수 있다. 이러한 광학적 파괴는 피하의 색소 관련 세포소기관을 파괴하거나 피하에 미세 손상 영역을 만들어 피부 재생 효과를 유도할 수 있다. 하지만 회절 광학 소자 및 마이크로 렌즈 어레이를 이용한 피코초 엔디야그 레이저 치료의 단점으로 비균일한 광 손상 영역을 만들어 내거나 침투 깊이가 얕아 깊은 진피층에 광 손상을 일으키지 못한다는 점이 있었다. 피부 병변의 종류와 병변의 경과에 따라 치료 영역을 달리해야 함에 있어서, 목표로 하는 피하 깊이와 특정 영역에 정밀한 치료가 가능하게 해야 할 필요성이 있다. 따라서 본 연구에서는 피부의 특정 깊이별로 레이저 빔을 전달하여 균일한 광 손상

영역을 만들어 낼 수 있는 광학 요소의 개발 연구를 진행하였다. 회절 광학 소자는 균일한 손상영역을 형성할 수 있었으나, 얇은 침투 깊이를 보였고, 마이크로 렌즈 어레이는 레이저를 깊이 침투시킬 수 있는 반면 비균일한 광 손상영역을 보이는 데 있어서 두 개의 광학 요소를 조합하여 장점들을 구현해보고자 하였다. 두 광학 요소로 조합된 시스템을 회절 렌즈 어레이(Diffractive lens array, DLA)라고 명명하였으며, 광학 시뮬레이션 프로그램(Zemax) 및 빔 프로파일러를 통해 기존 광학 소자들과 광학적 특성을 비교 분석하였다. 회절 렌즈 어레이는 광학 시뮬레이션과 빔프로파일 관찰에서 균일한 마이크로 빔 분포를 보였다. 회절 광학 소자에 비해 마이크로 빔의 크기는 컷으며, 마이크로 빔의 수는 같았다. 마이크로 렌즈 어레이는 가우시안 빔 분포를 보였으며, 중앙의 레이저 빔이 회절 렌즈 어레이와 회절 광학 소자보다 강하게 관찰되었다. 이어 조직에 대한 반응을 확인하기 위해 생체 외 돼지 피부의 표면에 일정한 에너지로 조사하고 조직학적 분석을 수행하였다. 회절 광학 소자와 마이크로 렌즈 어레이의 경우, 공통적으로 피하에 공포(vacuole)가 형성된 것을 확인할 수 있었으며, 회절 렌즈 어레이는 조직이 찢어진 형태의 열 파괴(Thermal Disruption)가 관찰되었다. 이러한 미세 손상 영역은 회절 렌즈 어레이의 초점 거리를 조절함에 따라 손상 영역의 깊이를 제어할 수 있었으며 표피, 유두 진피(Papillary dermis), 망상 진피(Reticular dermis)에 균일한 손상 영역을 형성할 수 있었다. 본 연구를 통해 달성하고자 하였던 균일한 손상영역과 깊이 조절의 성능은 확인할 수 있었으나, 생체 외 조직에 대한 반응으로 임상적 유효성을 다루기에 한계가 있다. 이후 실험을 통해 생체 내 조직에 대한 반응과 시술 경과에 따른 안전성, 유효성을 평가할 필요가 있으며, 더 나아가 레이저의 세기, 시술 주기, 시술 반복 횟수 등 피부 병변 별 레이저 치료 프로토콜을 최적화할 필요가 있다.

Table of contents

List of Figures	iv
List of Tables	v
Chapter 1. Introduction	1
Chapter 2. Materials and methods.....	7
2.1 Light Source.....	7
2.2 Laser beam simulation	8
2.3 Detection of beam profiles.....	9
2.4 Ex vivo experiments.....	9
Chapter 3. Results	11
3.1. Beam profile simulation.....	11
3.2. Beam profile detection.....	12
3.3. Histological analysis	14
3.4. DLA evaluations	18
Chapter 4. Discussion	22
Chapter 5. Conclusion.....	25
Chapter 6. Further directions	26
Chapter 7. References	29
Acknowledgment	32

List of Figures

- Figure 1.** Absorption coefficient as a function of wavelength for several tissue constituents.....1
- Figure 2.** Schematic handpiece designs with three optical elements: (a) DOE, (b) MLA, and (c) DLA. Picosecond Nd:YAG laser light (red arrows) was perpendicularly incident on the skin tissue surface. Note that each tissue demonstrates the corresponding beam profile (DOE = diffractive optical elements; MLA = micro-lens array; DLA = diffractive micro-lens array; FL = focal lens; BP = beam profile).....6
- Figure 3.** Numerical simulations (a and b) and corresponding beam profiles (c and d) of DOE, MLA, and DLA : (a) simulated beam patterns at focal plane, (b) cross-sectional view of irradiance along line (a'-a'') in (a), (c) measured beam profiles at focal plane, and (d) cross-sectional view of irradiance along line (c'-c'') in (c).....13
- Figure 4.** Histological analysis of porcine skin tissue after picosecond Nd:YAG laser irradiation with DOE, MLA, and DLA: Picosecond Nd:YAG laser light was incident perpendicularly on the skin tissue surface with each optical element beam profile (red in top images; 40X). Note that the yellow solid lines in H&E-stained histological images (bottom; 200X) represent laser-induced vacuoles (V) by DOE and MLA and thermal decomposition (TD) by DLA, respectively.....15
- Figure 5.** Quantitative comparison of maximum penetration depth (MPD in μm) in porcine skin tissue after picosecond laser treatment with DOE, MLA, and DLA (* $p < 0.05$ DOE vs. MLA; *** $p < 0.001$ DLA vs. DOE and MLA).....17
- Figure 6.** Quantitative analysis of porcine skin tissues after DLA-assisted laser irradiation at various focal depths (FD): (a) H&E-stained histological images (40X) captured at various FDs (0, 2, 4, and 6 mm). Yellow dotted areas represent laser-induced thermal decomposition (TD) in tissue. (b) Quantitative analysis on penetration depth of TD for each FD measured from histological images (N = 20). Note that different background colors in (b) represent various skin layers (E = epidermis; PD = papillary dermis; ID = intermediate region of the dermis; RD = reticular dermis).....19
- Figure 7.** Quantitative comparison of thermal decomposition (TD) area as function of TD penetration depth: (a) Focal depth (FD) = 0 mm, (b) FD = 2 mm, (c) FD = 4 mm, and (d) FD = 6 mm. Note that different background colors represent various skin layers (E = epidermis; PD = papillary dermis; ID = Intermediate region of the dermis; RD = reticular dermis).....21

List of Tables

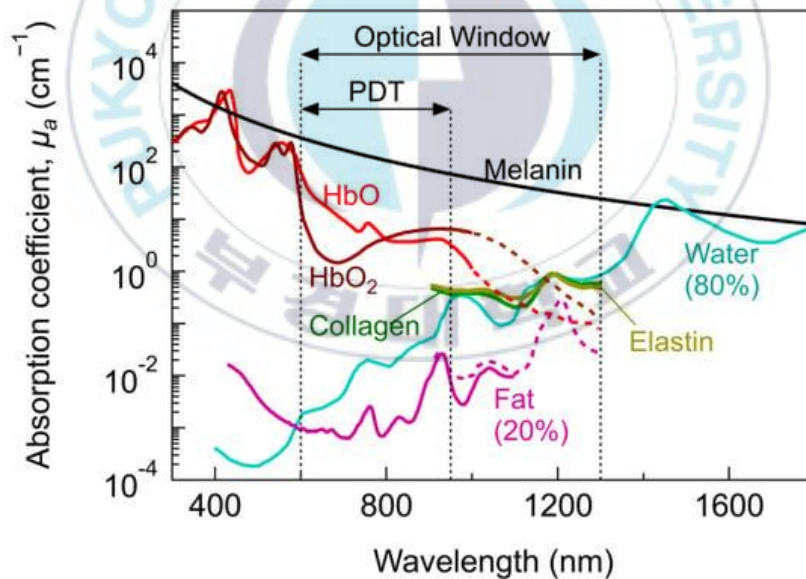
Table 1. Laser wavelength and clinical indications in dermatology.....2

Table 2. Thermal relaxation times of skin structures.....3



Chapter 1. Introduction

Lasers are widely used in modern medicine as they can non-invasively selectively absorb energy to specific tissues and cause tissue destruction or photochemical reactions. The lasers have the selectivity to damage or destroy only the target tissue depending on the wavelength, and the safety to preserve the surrounding normal skin tissue. Based on these characteristics, laser treatments targeting melanin, water, and blood vessels are performed in dermatology. As shown in Figure 1, the absorption coefficients of tissues are different for each wavelength [1].



[Figure adopted from Ref. (Algorri, José Francisco, et al. "Light technology for efficient and effective photodynamic therapy: a critical review." *Cancers* 13.14 (2021): 3484.)]

Figure 1. Absorption coefficient as a function of wavelength for several tissue constituents

532nm laser which has a high absorption coefficient for hemoglobin, can be used for vascular lesions treatment. In this way, various lasers are used in dermatology (Table 1) [2, 3].

Table 1. Laser wavelength and clinical indications in dermatology

Wavelength	Clinical Indication
418/514 nm	Vascular lesions
510 nm	Pigmented lesions
532 nm	Vascular lesions, pigmented lesions, red/orange/yellow tattoos
577/585 nm	Vascular lesions
585/595 nm	Vascular lesions, hypertrophic/keloid scars, striae, verrucae, nonablative dermal remodeling
694 nm	Hair removal, Pigmented lesions, blue/black/green tattoos
755 nm	Pigmented lesions, blue/black/green tattoos, hair removal, leg veins
800 ~ 810 nm	Hair removal, leg veins
1064 nm	Pigmented lesions, blue/black tattoos, hair removal, leg veins, nonablative dermal remodeling
1320 nm	Nonablative dermal remodeling
1450 nm	Nonablative dermal remodeling
1540 nm	Nonablative dermal remodeling
2490 nm	Ablative skin resurfacing, epidermal lesions
10,600 nm	Ablative skin resurfacing, epidermal/dermal lesions

Recently, with the growth of the aesthetic market, pigment treatments using laser are being performed. The representative laser is a Nd:YAG laser which have 1064nm wavelength. The 1064 nm wavelength has advantages in that it has a high absorption coefficient for melanin and can treat the dermis with a deep penetration depth. However, clinical effectiveness cannot be ensured only by selecting the wavelength.

One of the important parameters in laser treatment is the laser pulse duration. The pulse duration is the time interval during which laser energy is applied to the target tissue during one laser shot. Each laser has different pulse duration and the pulse duration range is from milliseconds to femtoseconds. In general, 1064nm laser with a range of several nanoseconds to several hundreds of picoseconds is used to treat skin pigments, and these are Q-switched Nd:YAG Laser and picosecond Nd:YAG Laser, respectively. The use of both lasers is related to the thermal relaxation time (TRT) of the pigment-related skin structures (Table 2) [4].

Table 2. Thermal relaxation times of skin structures

Structure	Size(μm)	Thermal relaxation time (approx.)
Melanosome cell	0.5 ⁻¹	1 μs
	10	300 μs
	50	1 ms
Tattoo particle	0.1	10 ns
Hair follicle	200	20 ms
Blood vessel	100	5 ms
Epidermis	50	1 ms
Erythrocyte	7	20 μs

The laser pulse duration within the TRT allows delivery of the laser energy without dispersing it to the surrounding tissue. Therefore, Q-switched Nd:YAG Laser and picosecond Nd:YAG Laser with pulse duration shorter than the TRT of melanosome cells are used for skin pigment treatment.

Picosecond Nd:YAG laser with a very short pulse duration (several hundred picoseconds) and a high peak power has widely been used in dermatology for treatment of pigmented lesions, resurfacing, and skin rejuvenation [5, 6]. The laser can deliver optical energy to target chromophores with no or minimal damage to the surrounding tissue because of selective photopyrolysis. To achieve the selective photothermolysis, the wavelength of laser should be preferentially absorbed by the target chromophores. The picosecond Nd:YAG laser can irradiate 1064 nm light on the skin to target the specific chromophores, such as melanin, hemoglobin, and water [7, 8]. In addition, the laser pulse duration is as important as the wavelength for the target chromophores to prevent the diffusion of thermal energy into the surrounding tissue. In order to minimize collateral damage to the surrounding tissue and to deliver light energy intensively to the target chromophore, the pulse duration should be equal to or shorter than the thermal relaxation time (TRT) of the target chromophores [9]. Thus, the pulse duration of several hundred picoseconds is 100-fold shorter than TRT of the skin chromophores (~50 ns), leading to effective ablation and no or minimal thermal injury in the skin. For effective skin treatment, picosecond Nd:YAG laser light is often used with optical elements, such as diffractive optical element (DOE) and micro lens array (MLA) [10-12]. The purpose of using DOE or MLA is the application of multiple micro-beams with high power density on skin. The multiple micro-beams induce cavitation (or vacuoles) in the epidermis and dermis [13-15]. The laser-induced vacuolization can generate micro-injury in the skin, and clinical evidences have reported skin rejuvenation resulting from the application of the micro-injury [16, 17]. However, the

picosecond Nd:YAG laser treatment using DOE and MLA still suffers from a difficulty of treating the deeper regions of the skin (DOE) or entailing a uniform distribution of the vacuolization (MLA). Our previous study reported that DOE induced vacuolization merely up to 400 μm below skin surface (near the basal membrane). In the case of MLA, the vacuoles were formed deeper in the skin (around 700 μm), but their spatial distribution was non-uniform (Gaussian-like) in the treated region [18, 19].

The goal of the current research was to develop a new optical element, diffractive micro-lens array (DLA), that enables deep and uniform laser treatment of pigments in a multi-layered skin tissue. As aforementioned, DOE and MLA suffer from shallow treatment depth and less uniform treatment, respectively. It is thus hypothesized that the combined features from DOE and MLA may obtain uniform and deep laser treatment of subcutaneous pigments at various depths in the skin to improve clinical outcomes. Figure 2 illustrates the schematics of handpiece designs with three optical elements: (a) DOE, (b) MLA, and (c) DLA (combination of DOE and MLA). The performance of the three optical elements was analyzed in terms of optical simulations, macro-beam patterns, and micro-beam distributions. Ex vivo skin tissue was tested with picosecond Nd:YAG laser light by using the three optical elements, and histological analysis was conducted to elucidate the optical and thermal responses of the tissue to the three optical elements.

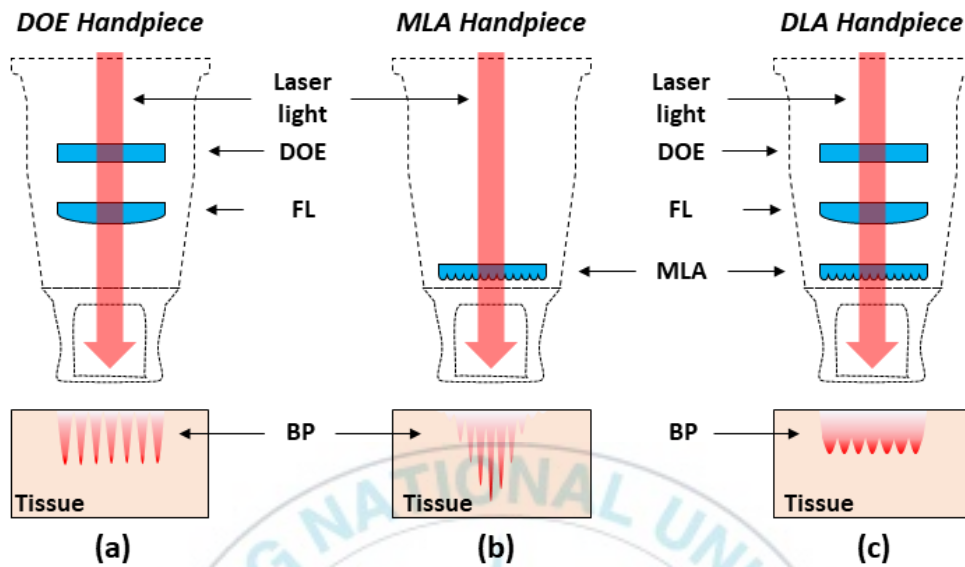


Figure 2. Schematic handpiece designs with three optical elements: (a) DOE, (b) MLA, and (c) DLA. Picosecond Nd:YAG laser light (red arrows) was perpendicularly incident on the skin tissue surface. Note that each tissue demonstrates the corresponding beam profile (DOE = diffractive optical elements; MLA = micro-lens array; DLA = diffractive micro-lens array; FL = focal lens; BP = beam profile).

Chapter 2. Materials and methods

2.1 Light Source

For experiments, picosecond Nd:YAG laser (wavelength = 1064 nm, pulse duration = 450 ps at full width at half maximum (FWHM); Picore, Bluecore Company, Busan, Republic of Korea) was used with three different handpieces: diffractive optical element (DOE; fused silica, macro-beam size = 4 mm in rectangular shape, micro-beam diameter (at image plane) = 165 μm , 49 micro-beams, focal length = 40 mm; Bluecore Company, Busan, Republic of Korea), micro-lens array (MLA; fused silica, macro-beam diameter = 4 mm in circular shape, micro-beam diameter (at image plane) = 220 μm , 37 micro-beams, focal length = 38.6 mm; Bluecore Company, Busan, Republic of Korea) handpiece, and diffractive micro-lens array (DLA). The DLA handpiece consisted of a combination of DOE and MLA and had variable focal depths (FDs) from the tip of the handpiece ranging from 0 (direct contact) to 6 mm. The picosecond laser system component had an articulated arm that delivered laser beam to a target tissue. Each hand-piece was mounted on the end of the articulated arm. The applied irradiances were 5.6 GW/cm^2 for DOE and DLA and 7.1 GW/cm^2 for MLA (single pulse energy = 400 mJ with stability of $\geq 90\%$). The corresponding fluences were 2.5 J/cm^2 for DOE and DLA and 3.1 J/cm^2 for MLA. It should be noted that MLA yielded a slightly higher fluence than DOE and DLA because of the smaller beam area (i.e., circle). A pyroelectric energy sensor (PE50BF-DIF-C, Ophir, Jerusalem, Israel) in conjunction with an energy meter (Vega, Ophir, Jerusalem, Israel) was used for energy calibration

prior to each experiment in order to minimize any experimental errors. Figure 2 presents schematic handpiece designs using three optical elements: (a) DOE, (b) MLA, and (c) DLA. The red regions in tissue represent the corresponding beam profiles from the handpieces.

2.2 Laser beam simulation

A spatial distribution of the laser beam from each handpiece was simulated by using an optical design program (ZEMAX 13 release 2/premium, Non-Sequential Mode, Kirkland, WA, USA). The optical simulation was performed to estimate the laser beam profiles observed at the distance corresponding to the length of the handpiece. In the simulation, the wavelength of the light source was 1064 nm. The arrangement and specifications of an optical system were set based on focal lengths and the measured distance between optical elements (DOE and MLA; fused silica) and a focal lens (N-BK7). The parameters for DOE were calculated by following the HOLO/OR LTD's tutorial on the Design and integration of 1D and 2D diffractive beam splitters (multi-spot) into optical systems in sequential and non-sequential modes of ZEMAX. A MS-219-I-Y-A (HOLO/OR) product was used to have a grating period (Λ) of 86.902 μm and a line/ μm ($1/\Lambda$) of 0.012. For MLA, a spherical lens (focal length = 38.6 mm) with Extruded in Object Type section of Non-Sequential Mode was used to make a hexagonal micro-lens. The hexagonal lens was thus combined with both Boolean and Array functions to create the micro-lens array. DLA was constructed by arranging DOE and MLA in line on the optical pathway. DOE was positioned first in the optical

pathway, the focal length was corrected with a plano-convex lens, and MLA was positioned last. Finally, a rectangular detector was employed in the simulated system in order to acquire the laser beam profiles through the Detector Viewer window.

2.3 Detection of beam profiles

To verify optical simulation results, laser beam profile was detected with three handpieces. Each handpiece was horizontally positioned, and both a neutral density filter (LBP2-ND3, 0.05-2% Transmission, Newport Corporation, CA, USA) and a laser beam profiler (LBP2-HR-VIS3, 190-1100 nm Silicon CCD, 1624×1224 Pixels, Newport Corporation, CA, USA) were situated at the end of the handpiece. The applied pulse energy was set at 1 mJ (fluence = 8 mJ/cm²) to prevent any color saturation in the acquired beam images.

2.4. *Ex vivo* experiments

For Dark pigmented porcine skin samples (Minipig; age = 4 months; weight = 16-20 kg) were procured from CRONEX Corp. (Hwaseong, Republic of Korea) to evaluate tissue responses to picosecond laser with three handpieces (DOE, MLA and DLA) in ex vivo model. The flesh skin samples were prepared by storing in an insulated box with ice the day after euthanasia. The tissue samples were sectioned in 25 × 25 mm² with 7 to 10 mm in thickness. Prior to laser irradiation, each handpiece was positioned vertically to the sectioned tissue surface. The macro-beam size was 4 × 4 mm² in a square shape (DOE and DLA) and 4 mm in diameter (MLA). The applied laser fluences

were 2.5 J/cm² for DOE and DLA and 3.1 J/cm² for MLA, and a single shot was applied for the laser treatment. The laser irradiation with each handpiece was repeated five times (N = 5). In the case of the DLA handpiece, the effect of FD on the tissue was evaluated by applying four different FDs (0, 2, 4, and 6 mm) under the same irradiation condition.

Laser-irradiated skin tissues were harvested and fixed in a 10% neutral formalin solution (Sigma Aldrich, St. Louis, Missouri) for seven days. The tissues were embedded in paraffin blocks and sliced in ~6 μm thickness. For histological analysis, the tissues were stained with hematoxylin and eosin (HE). The stained tissue slides were evaluated by using an optical microscope (Leica DM500, Leica, Wetzlar, Germany) to observe various tissue responses to picosecond laser light with three handpieces qualitatively and quantitatively. The extent of irreversible thermal injury (vacuole or thermal disruption) in the tissue was quantified in terms of size and depth for comparison by using Image J (National Institute of Health, Bethesda, MD, USA).

Chapter 3. Results

3.1. Beam profile simulation

Figure 3(a) demonstrates the beam profiles emitted from three different handpieces (DOE, MLA, and DLA) acquired by optical simulations. Each beam profile was formed on the plane of the distal end of the handpiece. The beam profile of the DOE handpiece consisted of 49 micro-beams (7×7 dots) in a macro-beam ($4 \times 4 \text{ mm}^2$). Each micro-beam size was $100 \mu\text{m}$ in diameter and uniformly distributed. Unlike DOE, the MLA handpiece showed a total of 127 micro-beams (including all energy levels) in a circular macro-beam (diameter = 6.8 mm). The highest intensity of the micro-beams occurred at the center, but the micro-beam intensity gradually decreased and became the lowest at the margin of the MLA macro-beam. It was noted that the micro-beam size varied from $198 \mu\text{m}$ (center) to $149 \mu\text{m}$ (margin). The DLA handpiece showed a square macro-beam ($4.6 \times 4.6 \text{ mm}^2$) consisting of 49 micro-beams (7×7 dots) in a uniform distribution, similar to the DOE handpiece. However, each micro-beam size was $502 \mu\text{m}$ in diameter, which was larger than that from the DOE handpiece.

Figure 3(b) exhibits cross-sectional views of the beam profiles acquired from the lines (a'-a'') in Fig. 3(a). Both DOE and DLA handpieces showed a uniform distribution of micro-beams in an equivalent macro-beam size. However, the DOE micro-beams yielded two-fold higher irradiances (I in W/cm^2) in a narrower intensity distribution whereas the DLA micro-beams had lower irradiances in a wider distribution (i.e., larger micro-beam size with lower irradiance). The MLA handpiece demonstrated a Gaussian

distribution of the micro-beams, of which the maximum intensity occurred at the center. Although the micro-beam intensities were comparable between DOE and MLA (center), the MLA micro-beam size (center) was two-fold larger than the DOE micro-beam size. It should be noted that the red dashed lines in Fig. 3(b) represent the contours of the micro-beam irradiances.

3.2. Beam profile detection

Figures 3(c) and 3(d) present the actual beam profiles measured from three handpieces. Similar to Fig. 3(a), DOE handpiece showed a rectangular beam profile ($4 \times 4 \text{ mm}^2$) with 49 micro-beams (7×7 dots; size = $50 \text{ }\mu\text{m}$). MLA handpiece yielded a total of 37 micro-beams (size = $100 \text{ }\mu\text{m}$) in a circular macro-beam with a diameter of 4.8 mm. Compared to the simulation results, the smaller micro-beam size could result from application of low laser energy to prevent light saturation for the beam profile measurements. The difference between the number of micro-beams and the macro-beam size in the simulation occurred as the laser beams with low energy were hardly detected by the beam profiler. The DLA handpiece showed a square macro-beam pattern ($4.3 \times 4.3 \text{ mm}^2$) with a total of 48 micro-beams, and each micro-beam size was $500 \text{ }\mu\text{m}$. Both the simulations and the experimental measurements showed a good agreement on the spatial distributions of macro- and micro-beams (Figs. 3(b) and 3(d)).

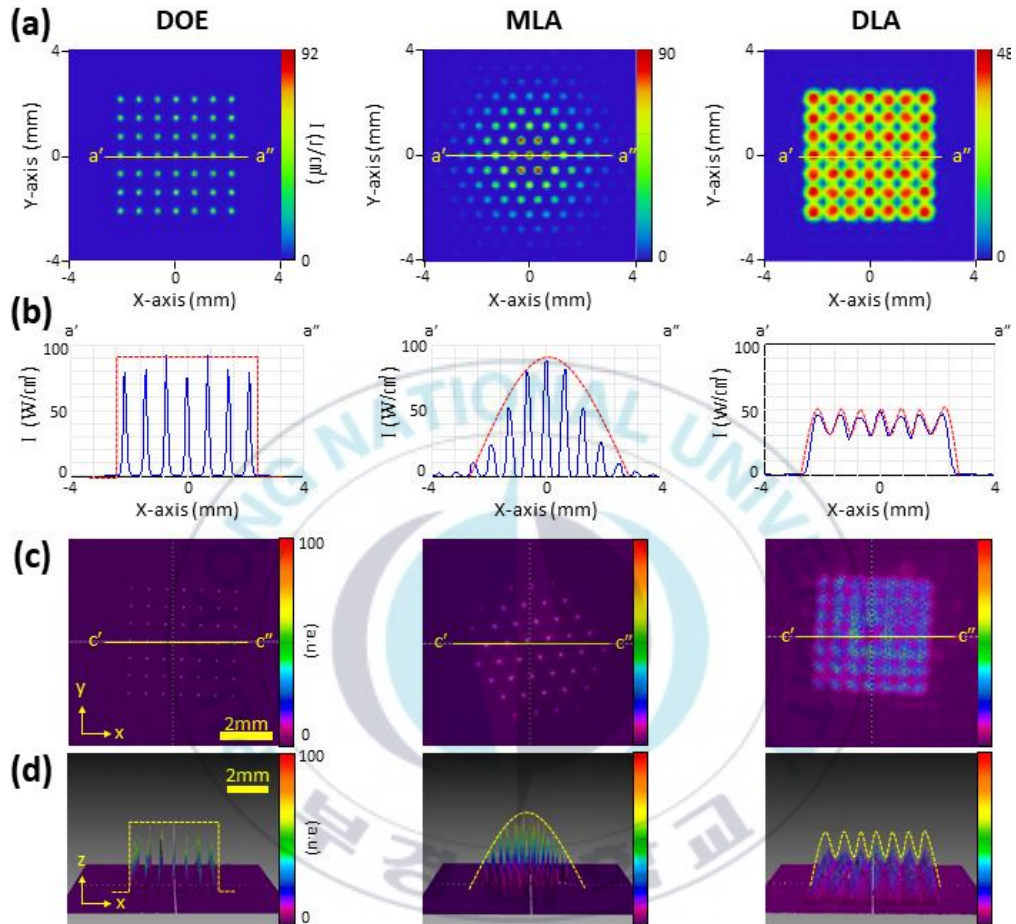


Figure 3. Numerical simulations (a and b) and corresponding beam profiles (c and d) of DOE, MLA, and DLA : (a) simulated beam patterns at focal plane, (b) cross-sectional view of irradiance along line ($a'-a''$) in (a), (c) measured beam profiles at focal plane, and (d) cross-sectional view of irradiance along line ($c'-c''$) in (c).

3.3. Histological analysis

Figure 4 shows HE-stained images of ex vivo porcine skin tissue after picosecond Nd:YAG laser irradiation with DOE, MLA and DLA. Both DOE and MLA handpieces induced vacuoles in the treated tissue. In the case of the DOE handpiece, the vacuoles were mainly created near the basal membrane in the epidermal layer without damage to the stratum corneum. The MLA handpiece presented noticeable thermal damage to the stratum corneum (partial surface ablation), but the formation of the vacuoles was deeply and widely distributed in the dermal layer. On the other hand, the DLA handpiece showed that the dermis was partially torn and discolored (dark purple regions) with no vacuolization. These histological features evidenced a result of laser-induced mechanical and thermal damage in the tissue, which was called as thermal disruption (TD) in the current study. It should be noted that the formation of the vacuoles (DOE and MLA) or TD (DLA) well corresponded to the spatial distributions of the incident laser beam, which is shown at the top of the images (red areas) in Fig. 4.

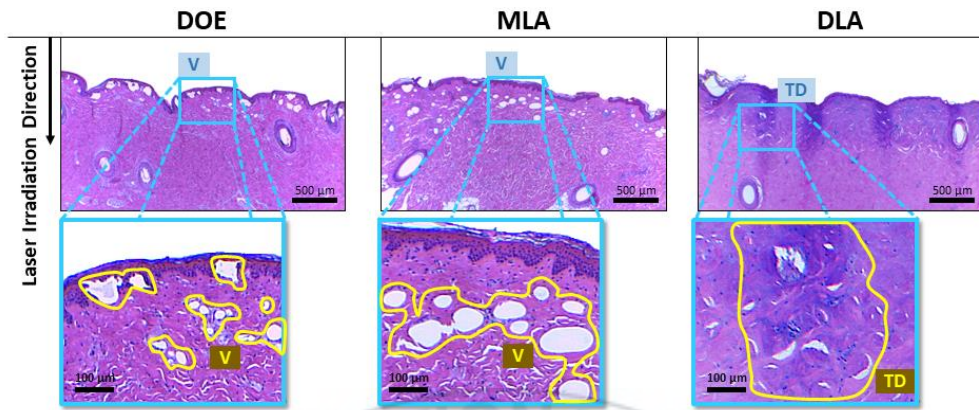


Figure 4. Histological analysis of porcine skin tissue after picosecond Nd:YAG laser irradiation with DOE, MLA, and DLA: Picosecond Nd:YAG laser light was incident perpendicularly on the skin tissue surface with each optical element beam profile (red in top images; 40X). Note that the yellow solid lines in H&E-stained histological images (bottom; 200X) represent laser-induced vacuoles (V) by DOE and MLA) and thermal decomposition (TD) by DLA, respectively.

Figure 5 quantitatively compares the maximum penetration depths (MPDs) of irreversible thermal injury (vacuoles for DOE and MLA and TD for DLA) in porcine skin tissue after picosecond laser treatment. The DOE handpiece created the smallest MPD in the skin ($305 \pm 75 \mu\text{m}$) while the MLA handpiece yielded a two-fold larger MPD than the DOE handpiece ($625 \pm 49 \mu\text{m}$; $p < 0.05$). On the other hand, the DLA handpiece (FD = 6 mm) generated the largest MPD of $1115 \pm 130 \mu\text{m}$ ($p < 0.001$ vs. DOE and MLA).



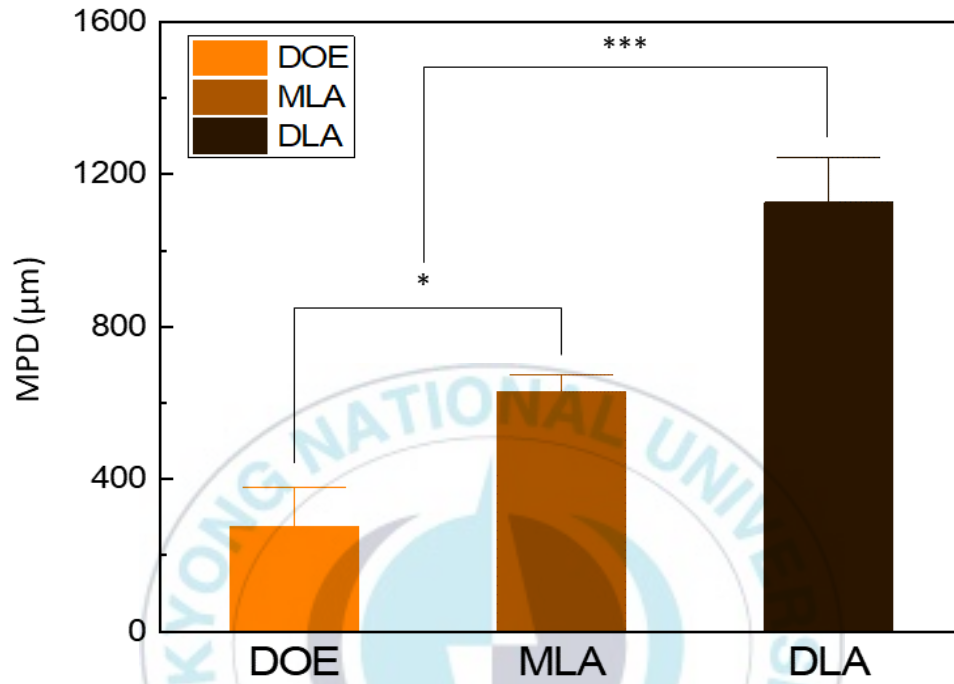


Figure 5. Quantitative comparison of maximum penetration depth (MPD in μm) in porcine skin tissue after picosecond laser treatment with DOE, MLA, and DLA ($p < 0.05$ DOE vs. MLA; $*** p < 0.001$ DLA vs. DOE and MLA).

3.4. DLA evaluations

Figure 6(a) shows HE-stained histological images (10×) of skin tissue after DLA-assisted laser treatment at various FDs. Yellow dashed lines represent the formation of TD in the tissue, which corresponded to the discolored region with the directional tissue disruption. Overall, the depth of the TD increased with FDs. FD = 0 mm created the shallowest TD solely in the epidermis (E) while FD = 6 mm induced the deepest TD distributed in the intermediate region of the dermis (ID) and reticular dermis (RD). Figure 6(b) quantifies the penetration depth of the TD at various FDs (N = 20 per FD). FD = 0 mm yielded the shallowest penetration of the TD ($57 \pm 21 \mu\text{m}$) with the minimal distribution in the epidermal layer. Similar to Fig. 6(a), the penetration depth gradually increased with FDs. When FD = 2 mm, the TD primarily occurred between papillary dermis (PD) and ID ($371 \pm 230 \mu\text{m}$). FDs of 4 mm and 6 mm entailed the TD in the ID ($587 \pm 261 \mu\text{m}$) and RD ($763 \pm 356 \mu\text{m}$), respectively. It was noted that FD = 6 mm created the deepest TD in a wider distribution in the tissue.

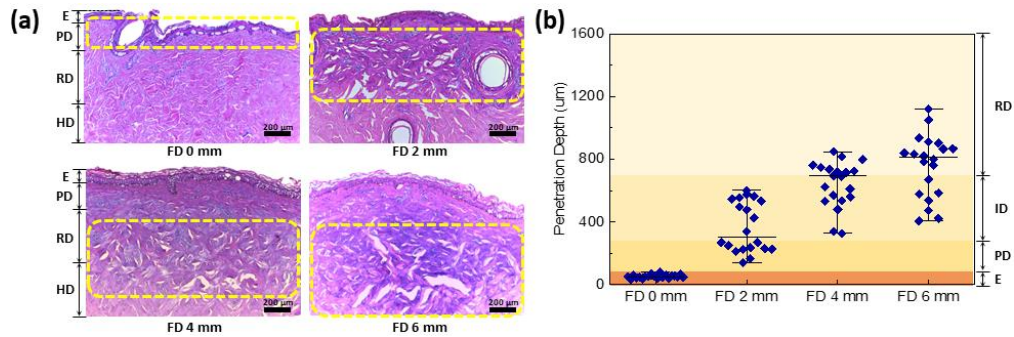


Figure 6. Quantitative analysis of porcine skin tissues after DLA-assisted laser irradiation at various focal depths (FD): (a) H&E-stained histological images (40X) captured at various FDs (0, 2, 4, and 6 mm). Yellow dotted areas represent laser-induced thermal decomposition (TD) in tissue. (b) Quantitative analysis on penetration depth of TD for each FD measured from histological images (N = 20). Note that different background colors in (b) represent various skin layers (E = epidermis; PD = papillary dermis; ID = intermediate region of the dermis; RD = reticular dermis).

Figure 7 shows a quantitative comparison of TD area as a function of TD depth at four different FDs. Evidently, the TD area increased with the TD depth. When $FD = 0$ mm, the TD with an average area of $269 \mu\text{m}^2$ was formed limitedly in the epidermal layer. $FD = 2$ mm distributed the TD with an average area of $284 \mu\text{m}^2$ over PD and ID. When $FD = 4$ mm, the TD with an average area of $436 \mu\text{m}^2$ was mostly generated in ID, and the partial TD was formed at the interface between ID and RD. $FD = 6$ mm created the largest TD area ($4,980 \mu\text{m}^2$), covering from PD to deep RD.



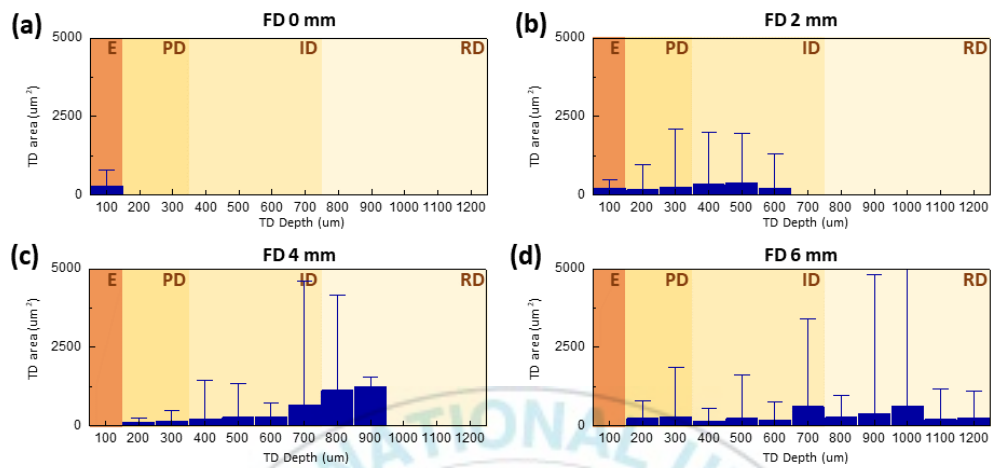


Figure 7. Quantitative comparison of thermal decomposition (TD) area as function of TD penetration depth: (a) Focal depth (FD) = 0 mm, (b) FD = 2 mm, (c) FD = 4 mm, and (d) FD = 6 mm. Note that different background colors represent various skin layers (E = epidermis; PD = papillary dermis; ID = Intermediate region of the dermis; RD = reticular dermis).

Chapter 4. Discussion

The current study designed a new DLA optical element to achieve multiple micro-beams in a uniform manner and to induce uniform micro-injury zones at various depths in multi-layered skin tissue. Both optical simulation and beam profile measurements validated that DLA formed multiple micro-beams, of which size was ten- and five-fold larger than those of DOE and MLA, respectively (Fig. 3). According to our previous study, DOE created vacuoles in a uniform manner at various FDs (0~5 mm). However, the vacuoles were hardly formed in the skin layer deeper than 400 μm possibly due to the limited beam collimation. In fact, the preliminary optical simulation confirmed that the beam distribution became diverging significantly beyond the focal plane, implicating that the optical breakdown was solely limited within the skin surface. Although MLA generated the vacuoles in the deeper skin layer (~930 μm), the distribution of the vacuoles was inherently Gaussian-like and no significant change in the penetration depth was observed with varying FDs. On the other hand, the current study demonstrated that DLA was able to create a uniform distribution of TD in the ex vivo skin and to control the TD location in a FD-dependent manner (0~6 mm). In addition, DLA could target the chromophores located in the deep skin layers by forming the extent of TD up to 1,115 μm in spite of a different type of micro-injury, compared to those of DOE and MLA. Therefore, DLA-assisted picosecond laser treatment can provide the combined features from DOE and MLA and may help obtain deep and uniform laser treatment at various depths in the skin for enhancing clinical outcomes.

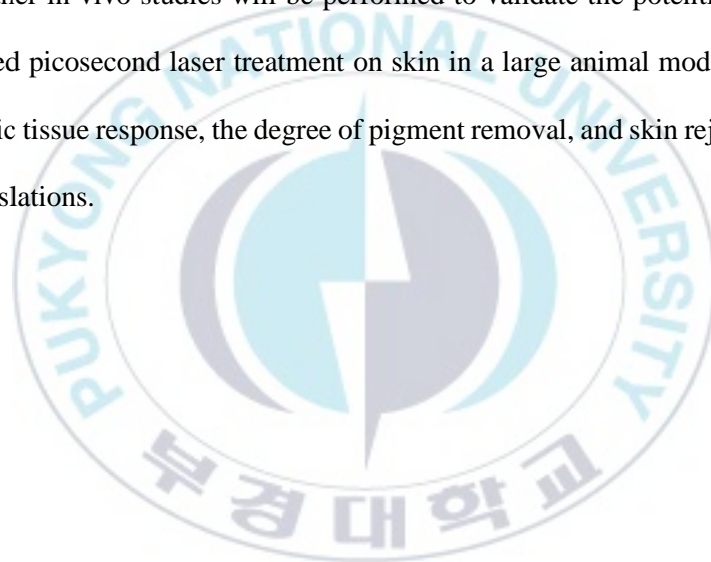
DLA entailed TD with skin tissue partially ripped and discolored whereas both DOE and MLA created evident vacuolization in the upper epidermal basal membrane (Fig. 4). In spite of a uniform distribution of micro-beams (Fig. 3), both mechanical and thermal micro-injury (i.e., TD) after DLA-assisted laser treatment could be associated with a large coverage of the DLA micro-beams. The current pulse duration (450 ps) is considerably shorter than TRT of skin chromophores (~50 ns), satisfying thermal confinements for laser treatment [20]. However, the larger DLA micro-beams could have decreased the incident irradiance inside the tissue, possibly mitigating the immediate development of laser-induced plasma with high pressure and temperature upon volumetric energy deposition. Instead, the targeted tissue volume could have undergone both partial pressure elevation (mechanical injury) and heat accumulation as well as conduction (thermal injury), resulting in the axial tissue rupture surrounded by irreversible thermal coagulation (Figs. 4 and 6) at various tissue depths. In fact, it was observed during the experiments that DLA-assisted laser irradiation formed plasma with noticeably weaker luminescence and lower pressure transient (less audible sound), compared to DOE- and MLA-assisted laser irradiation. However, the potential benefits of the combined micro-injury by generated by the DLA-assisted laser treatment still needs to be explored for clinical translations. Therefore, further studies will design and optimize the optical layouts for DLA in order to have a smaller micro-beam size for inducing vacuolization instead of TD inside the tissue during picosecond laser irradiation. In addition, the delayed response of the skin tissue to TD will be investigated to elucidate the effect of the combined (mechanical and thermal) micro-

injury after the DLA-assisted laser treatment on chronic inflammation, wound healing and repair, and collagen remodeling, compared with that of the skin to the vacuolization.

DLA-assisted picosecond laser irradiation could provide multiple treatment options, such as pigment removal, skin rejuvenation, and collagen remodeling, selectively at various skin layers and depths. Figure 6 shows that the location of the micro-injury (vacuoles or TD) formation seemed to be contingent upon FDs. Thus, it is conceived that the selective laser treatment of various skin layers could broaden clinical benefits. For instance, the DLA-assisted laser irradiation at FD = 0 mm yielded the vacuoles solely within the epidermal layer (~100 μm ; Fig. 6), implicating selective pigment destruction as a result of light absorption [21] by pigment-laden cells (melanocytes, keratinocytes, and naevus cells [4]) in E. Hence, the selective destruction of the pigment-laden cells can be instrumental in treating pigmented skin disease. On the other hand, the deeper FDs of 2 and 6 mm were able to generate micro-injury (TD) in PD (100~300 μm) and RD (700 μm ~), respectively (Fig. 6). The occurrence of the micro-injury could stimulate papillary and reticular fibroblasts in PD and RD, respectively, further activating collagen formation and remodeling in the skin [22, 23]. For clinical translations, further in vivo studies should be pursued in in vivo porcine models to evaluate the collagen remodeling and to validate the potential effects of the proposed treatment on PD and RD by means of visualization with polarized light microscopy, western blot analysis, and real-time PCR analysis.

Chapter 5. Conclusion

The current study designed and developed a new optical element of DLA by combining the features of DOE and MLA in order to achieve uniform and selective laser application for skin. Both a uniform distribution of micro-beams and a constant beam collimation from DLA could help generate TD in a uniform manner and at various skin depths. Further in vivo studies will be performed to validate the potential benefits of DLA-assisted picosecond laser treatment on skin in a large animal model in terms of acute/chronic tissue response, the degree of pigment removal, and skin rejuvenation for clinical translations.



Chapter 6. Further directions

DLA could provide uniform micro-beam distributions at various depths in skin, experimental limitations still remain. It was noted that the current optical simulation showed a 40% smaller DOE micro-beam diameter than the actual one (100 μm for simulation vs. 165 μm for measurement). A potential explanation for the discrepancy can be the application of the HOLO/OR LTD's tutorial using the different DOE specifications. Thus, in order to further optimize the performance of the proposed optical elements with optical simulations, the optical design for the actual DOE and MLA specifications should be developed. In spite of the uniform micro-beam array for DLA (7 \times 7), the rotational alignment of DOE and MLA in the same handpiece could still induce interference patterns (e.g., Moire pattern) because of different optical features. Thus, the alignment of the optical elements should be further optimized to minimize the interference patterns and to attain the uniform micro-beam array for DLA with smaller micro-beam diameters. Unlike DOE and MLA, DLA generated larger micro-beams with lower intensities (Fig. 3), which led to TD in the skin rather than vacuolization (Fig. 4). In spite of the uniform distribution of the micro-beams, DLA was a combination of DOE and MLA by increasing a DC component in the beam profile, which led to TD with the increased micro-beam diameter. Thus, further investigations will be followed to optimize the optical configurations of DLA to generate a smaller micro-beam size in a uniform micro-beam array with a capacity for variable focal depths. Thus, the smaller micro-beams could yield the uniformly localized vacuoles or

micro-injury zones at various skin depths, improving clinical efficacy and safety. In addition, in the case of the DOE and MLA handpieces, the focus of the micro-beams was close to the skin surface or superficial layer of the skin. If optical breakdown were dominant in E or PD, cavitation dynamics consumed most of the laser energy and worked as a shield against any further migration of photons into the deeper layer of the skin. In the case of picosecond laser, it can be conceived that all the energy was virtually expended in the optical breakdown and photoacoustic coupling (i.e. shockwave and cavitation) with minimal direct thermal contribution. Any subsequent thermal effects could be secondary to acoustic-thermal coupling. In order to deliver the incident laser energy deeper with more spatial control, these superficial disruptive events need to be minimized. Although the proposed method was to move FD of the DLA handpiece into ID and RD, the optical breakdown was minimized but photothermal coupling became more effective instead to produce the deeper lesions (Figs. 4 and 5). Alternatively, the position of the plano-convex lens focus in the DOE handpiece can also be adjusted to provide similar phenomena (i.e., dominant photothermal effect with deeper TD) to the DLA performance although the current study evaluated the feasibility of a combination of DOE and MLA. Thus, instead of the proposed combination, further design and quality of DOE should be performed to enhance a therapeutic capacity of selective picosecond laser treatment and its treatment outcomes in the skin. The current study used ex vivo porcine skin to compare the performance of three optical elements. In spite of quantitative validations, the ex vivo tissue hardly reflects human tissue because of different optical/thermal properties, no blood perfusion with convective heat transfer,

no metabolic heat generation [24]. In addition, the current findings merely demonstrated the acute response of the laser-treated tissue to the picosecond laser irradiation with DOE, MLA, and DLA. However, for clinical translations, the delayed tissue response should be investigated to confirm the development of micro-lesions, the degree of inflammation, wound healing, and collagen remodeling. Therefore, further in vivo large animal studies will be performed to validate the current ex vivo findings and to substantiate the potential clinical benefit of DLA in terms of acute/chronic tissue response, degree of pigment removal, and skin rejuvenation.



Chapter 7. References

- [1] J.F. Algorri, M. Ochoa, P. Roldán-Varona, L. Rodríguez-Cobo, J.M. López-Higuera, Light technology for efficient and effective photodynamic therapy: a critical review, *Cancers* 13(14) (2021) 3484.
- [2] E.L. Tanzi, J.R. Lupton, T.S. Alster, Lasers in dermatology: four decades of progress, *Journal of the American Academy of Dermatology* 49(1) (2003) 1-34.
- [3] S. Gianfaldoni, G. Tchernev, U. Wollina, M. Fioranelli, M.G. Rocchia, R. Gianfaldoni, T. Lotti, An overview of laser in dermatology: the past, the present and... the future (?), *Open access Macedonian journal of medical sciences* 5(4) (2017) 526.
- [4] B. Brazzini, G. Hautmann, I. Ghersetich, J. Hercogova, T. Lotti, *Laser tissue interaction in epidermal pigmented lesions*, Blackwell Science Ltd Oxford, UK, 2001, pp. 388-391.
- [5] Y.X. Dai, Y.Y. Chuang, P.Y. Chen, C.C. Chen, Efficacy and safety of ablative resurfacing with a high-energy 1,064 Nd-YAG picosecond-domain laser for the treatment of facial acne scars in Asians, *Lasers in Surgery and Medicine* 52(5) (2020) 389-395.
- [6] D.G. Kim, S.M. Nam, J.S. Shin, E.S. Park, Effectiveness of the pico-toning technique for the treatment of melasma with a low fluence 1,064-nm Nd: YAG laser in Asian patients, *Medical Lasers; Engineering, Basic Research, and Clinical Application* 9(2) (2020) 166-171.
- [7] L. Carroll, T.R. Humphreys, LASER-tissue interactions, *Clinics in dermatology* 24(1) (2006) 2-7.
- [8] N. Stewart, A.C. Lim, P.M. Lowe, G. Goodman, Lasers and laser-like devices: Part one, *Australasian Journal of Dermatology* 54(3) (2013) 173-183.
- [9] R.R. Anderson, J.A. Parrish, Selective photothermolysis: precise microsurgery by selective absorption of pulsed radiation, *Science* 220(4596) (1983) 524-527.

- [10] T.H.S. Wong, Picosecond Laser Treatment for Acquired Bilateral Nevus of Ota-like Macules, *JAMA dermatology* 154(10) (2018) 1226-1228.
- [11] C.H. Lee, E.M. Jin, H.S. Seo, T.-U. Ryu, S.P. Hong, Efficacy and safety of treatment with fractional 1,064-nm picosecond laser with diffractive optic element for wrinkles and acne scars: A clinical study, *Annals of Dermatology* 33(3) (2021) 254.
- [12] S. Palawisuth, W. Manuskiatti, C. Apinuntham, R. Wanitphakdeedecha, K.A.G. Cembrano, Quantitative assessment of the long-term efficacy and safety of a 1064-nm picosecond laser with fractionated microlens array in the treatment of enlarged pores in Asians: A case-control study, *Lasers in Surgery and Medicine* 54(3) (2022) 348-354.
- [13] H.J. Chung, H.C. Lee, J. Park, J. Childs, J. Hong, H. Kim, S.B. Cho, Pattern analysis of 532-and 1064-nm microlens array-type, picosecond-domain laser-induced tissue reactions in ex vivo human skin, *Lasers in Medical Science* 34(6) (2019) 1207-1215.
- [14] H.-J. Ahn, D.H. Suh, I.-H. Kang, S.J. Lee, M.K. Shin, K.Y. Song, Interaction of skin with fractional picosecond laser in Asian patients, *The Journal of Clinical and Aesthetic Dermatology* 14(11) (2021) 14.
- [15] M. Zhang, Y. Guan, Y. Huang, E. Zhang, T. Lin, Q. Wu, Histological Characteristics of Skin Treated With a Fractionated 1064-nm Nd: YAG Picosecond Laser With Holographic Optics, *Lasers in Surgery and Medicine* 53(8) (2021) 1073-1079.
- [16] L. Kirsanova, E. Araviiskaia, M. Rybakova, E. Sokolovsky, A. Bogantenkov, F. Al-Niaimi, Histological characterization of age-related skin changes following the use of picosecond laser: low vs high energy, *Dermatologic Therapy* 33(4) (2020) e13635.
- [17] C.S.M. Wong, M.W.M. Chan, S.Y.N. Shek, C.K. Yeung, H.H.L. Chan, Fractional 1064 nm picosecond laser in treatment of melasma and skin rejuvenation in Asians, a prospective study, *Lasers in Surgery and Medicine* 53(8) (2021) 1032-1042.

- [18] H. Kim, J.K. Hwang, M. Jung, J. Choi, H.W. Kang, Laser-induced optical breakdown effects of micro-lens arrays and diffractive optical elements on ex vivo porcine skin after 1064 nm picosecond laser irradiation, *Biomedical Optics Express* 11(12) (2020) 7286-7298.
- [19] H. Kim, J.K. Hwang, J. Choi, H.W. Kang, Dependence of laser-induced optical breakdown on skin type during 1064 nm picosecond laser treatment, *Journal of Biophotonics* 14(9) (2021) e202100129.
- [20] M.F. Yang, V.V. Tuchin, A.N. Yaroslavsky, Principles of light-skin interactions, *Light-Based Therapies for Skin of Color*, Springer2009, pp. 1-44.
- [21] D.J. Goldberg, Laser treatment of pigmented lesions, *Dermatologic clinics* 15(3) (1997) 397-407.
- [22] M. Takeo, W. Lee, M. Ito, Wound healing and skin regeneration, *Cold Spring Harbor perspectives in medicine* 5(1) (2015) a023267.
- [23] D.M. Reilly, J. Lozano, Skin collagen through the lifestages: Importance for skin health and beauty, *Plastic and Aesthetic Research* 8 (2021) 2.
- [24] M.H. Niemz, Interaction mechanisms, *Laser-Tissue Interactions*, Springer2002, pp. 45-149.

Acknowledgment

약 2 년간의 석사과정을 마치고 학위 논문을 제출하게 되었습니다. 그 동안 주변 동료들, 교수님들의 가르침과 조언, 격려가 있었기에 가능했던 일인 것 같습니다. 미흡하지만 학위 논문을 마치면서 감사의 말씀을 전합니다.

먼저 연구의 방향성과 성과의 활용방안 등을 제시해주시고 지도해 주셨던 강현욱 교수님께 진심으로 감사드립니다. 많은 가르침을 받았다고 생각되지만 여전히 교수님과 대화 한마디 한마디에 배울 점이 많다고 느껴집니다. 금번 석사과정간의 가르침들을 디딤돌 삼아 끊임없이 정진할 수 있도록 노력하겠습니다.

바쁘신 와중에도 학위 논문심사에 참여해주시고 격려해주신 오정환 교수님, 이명기 교수님, 석사과정간 관련 전공 지식을 교육해주신 이병일 교수님, 정원교 교수님께도 깊은 감사의 말씀을 전합니다.

비교적 늦은 시기에 대학원에 입학하게 되어 홀로 적응하기 어려웠을 텐데, 함께 있던 Bio Ablation Lab 친구, 후배들이 있었기에 큰 어려움없이 헤쳐올 수 있었던 것 같습니다. 아낌없이 지원해주고 조언해주었던 김혜진 박사님, 스스로없이 대해주고 도와주었던 이예찬 후배님, 임성희 후배님, 이지호 후배님, 신화랑 후배님에게도 감사하다는 말을 전하고 싶습니다.

석사 과정을 권유해주시고 아낌없는 응원과 지원을 해 주신 블루코어컴퍼니 김성민 대표님, 정재현 부사장님, 이현욱 연구소장님, 주이삭 차장님께도 진심으로 감사드립니다.

죽마고우 김상원, 김종우, 송창섭, 신승민, 김준승, 그리고 부경대학교 의공학과 동기 양철현, 문민규, 오랫동안 저의 주변에서 변함없이 함께해준 그들이 있었기에 잠시 힘들거나 지칠 때도 웃을 수 있었던 것 같습니다.

사랑하는 저의 가족, 아버지, 어머니, 동생 상아의 관심과 격려가 있었기에 포기하지 않고 해낼 수 있었던 것 같습니다. 그 관심과 격려에 감사의 말씀을 전합니다. 마지막으로 저의 옆에서 항상 응원해주고 제 노력을 지지해주었던 저의 예비 신부 황지은에게 고맙고 사랑한다는 말을 전합니다.

여전히 배울 것이 많고 부족한 저이지만 이번 석사학위를 발판삼아 더 성장해 나갈 수 있도록 하겠습니다.

최종만 올림